



ORIGINAL ARTICLE

Stress distribution of two commercial dental implant systems: A three-dimensional finite element analysis



Hao-Sheng Chang^{a,b}, Yi-Chin Chen^c, Yao-Dung Hsieh^{a,d},
Ming-Lun Hsu^{e*}

^a Department of Dentistry, Kaohsiung Veterans General Hospital, Taiwan

^b Shu Zen College of Medicine and Management, Kaohsiung, Taiwan

^c Medical Device and Opto-electronics Equipment Department, Metal Industries, Research and Development Center, Kaohsiung, Taiwan

^d School of Dentistry, National Defense National Medical Center, Taipei, Taiwan

^e Department of Dentistry, National Yang Ming University, Taipei, Taiwan

Received 5 January 2012; Final revision received 15 March 2012

Available online 11 May 2013

KEYWORDS

dental implant;
finite element
analysis;
platform switching

Abstract *Background/purpose:* This study investigates the stress distributions in an implant, abutment, and crown restoration with different implant systems, in various bone qualities, and with different loading protocols using a three-dimensional finite element model.

Materials and methods: Eight three-dimensional finite element models with 16 test conditions containing four types of dental implants embedded in two different bone qualities (types II and IV) under 100-N axial and 30° oblique loading forces were applied to analyze the stress distribution in the crown restoration, abutment, abutment screw, implant, and supporting bone.

Results: The highest maximum von Mises stress was noted in the abutment of a tissue-level implant with the Straumann system (1203.04 MPa) under a 30° oblique loading force. With axial load application, stresses in the screw and abutment of the NobelBiocare system were greater in the tissue-level implant (MK III) than in the bone-level implant (Active). The von Mises stresses in the cortical bone were mostly greater in the tissue-level implant (MK III) than in the bone-level implant (Active) of the NobelBiocare system. However, von Mises stresses in cancellous bone were mostly greater in the bone-level implant (Active) than in the tissue-level implant (MK III) of the NobelBiocare system.

Conclusion: Within the limitations of the present study, the Straumann system produced greater stresses than the NobelBiocare system in type IV cortical bone, but they were almost

* Corresponding author. Department of Dentistry, National Yang-Ming University, 155 Li-Nong Street, Section 2, Taipei, 112 Taiwan.
E-mail address: mlhsu@ym.edu.tw (M.-L. Hsu).

equal in type II bone. By contrast, the NobelBiocare system produced greater stresses than the Straumann system in cancellous bone, regardless of the type of loading angle or bone quality. Copyright © 2013, Association for Dental Sciences of the Republic of China. Published by Elsevier Taiwan LLC. All rights reserved.

Introduction

In spite of dental implants having been successfully used to restore the function of missing teeth in partially and completely edentulous patients,^{1,2} loss of osseointegration still sometimes occurs.³ Investigating the stress distribution can provide important information for implant design and optimizing implant placement for various types of bone quality.^{4,5} Bone quality is well accepted as one of the key factors affecting the long-term success of dental implants. Several studies have suggested that poor bone quality exhibits the greatest failure rates because of a thin cortical bone and low-density cancellous bone with a poor capability to react properly to stresses generated by occlusal loads, and is especially correlated with cases of single implants and high crown-root ratios.⁶

In contrast to natural teeth, there is no periodontal ligament between a dental implant and the surrounding bone, and the poor capacity for detection of biting forces may increase the tendency for occlusal overloading which can result in peri-implant bone loss and implant failure.⁷ Occlusal overloading is usually caused by premature contact between the implant-retained crown and opposing natural teeth or even implant prostheses. Some animal studies investigated the influence of occlusal overloading on the bone around dental implants. Results of those studies revealed that occlusal overloading could be a very important factor in loss of osseointegration of dental implants.^{7,8}

Another interesting issue is the prosthetic concept of platform switching, which has been introduced to the market recently and also has been studied histologically in both animals and humans.⁹ Although many studies have reported the benefits of platform switching correlated with biological or biomechanical situations,^{10–13} information from studies with long-term observations is still lacking. Furthermore, it is still not known whether marginal bone level alterations are affected by the extent of implant–abutment mismatching.¹⁴ The objective of this study was to analyze the stress distribution in two popular commercial dental implant systems, containing different collar designs, with three-dimensional (3D) finite element models, which

were performed using different bone qualities and different loading protocols.

Materials and methods

Eight 3D finite element models were built with SolidWorks 2011 software (SolidWorks Corporation, Concord, MA, USA) and Abaqus 6.9 software (SIMULIA Corporation, Providence, RI, USA) to analyze stress distributions. Each set of the model contained a crown, cement-type abutment, implant, and abutment screw, which received a 35-N preload. A 100-N axial force and a 30° oblique loading force were applied to the occlusal table of the crown restoration to analyze stress distributions in the crown, abutment, abutment screw, implant, and supporting bone.

Implant systems

NobelBiocare system

A Brånemark MKIII TiU RP implant (length = 11.5 mm, external collar diameter = 4.1 mm; Nobel Biocare, Göteborg, Sweden) was connected to a screw-retained, external hexagonal abutment (length = 7.5 mm, diameter = 4.1 mm; Nobel Biocare) with a straight margin connection. The NobelActive RP bone-leveled implant (length = 10 mm, external collar diameter = 3.9 mm; Nobel Biocare) was connected to a screw-retained, internal hexagonal abutment (length = 6.5 mm, implant interface diameter = 3.4 mm; Nobel Biocare) with a 0.25-mm convergent implant collar platform.

Straumann system

A Straumann SLA tissue-leveled standard plus implant (length = 10 mm, external collar diameter = 4.8 mm; Straumann, Basel, Switzerland) connected to a screw-retained, internal hexagonal abutment (length = 6 mm, diameter = 4.5 mm, straight standard abutment; Straumann, Basel, Switzerland) with a divergent match margin connection. The Straumann SLA bone-leveled implant (length = 10 mm, external diameter = 4.1 mm; Straumann, Basel, Switzerland) connected to a screw-retained

Table 1 Physical properties of the different components used in this study.^{15,16}

Component	Elastic modulus (GPa)	Poisson ratio	Source
Cortical bone	13.0	0.3	Tada et al ¹⁷
Cancellous bone			
High density	1.37	0.3	Sevimay et al ¹⁸
Low density	0.8	0.3	Tepper et al ¹⁹
Titanium (implant, abutment, screw)	102	0.3	Tada et al ¹⁷
Crown (gold alloy)	95	0.3	Craig ²⁰

internal hexagonal abutment (length = 6 mm, implant interface diameter = 3.5 mm, straight standard abutment; Straumann, Basel, Switzerland) with a 0.3 mm convergent implant collar platform.

Material properties

All of the materials used in this study were considered to be homogenous, isotropic, and linearly elastic. The physical properties of different components modeled in this study are illustrated in Table 1.^{15,16} The implant, abutment, and abutment screw were all designed to be titanium alloy with an elastic modulus of 102.0 GPa.¹⁷ Two types of bone density were modeled by varying the elastic modulus of compact bone and cancellous bone (with high and low densities) with elastic moduli of 13.0 GPa, 1.37 GPa, and 0.8 GPa, respectively.^{17–19} A gold alloy crown restoration is usually used for implant rehabilitation at the posterior region, and the superstructure for the model was designed to be an 86% gold alloy restoration with an elastic modulus of 95 GPa.²⁰

Model design and interface conditions

Each set of the model containing the gold alloy crown, cement-type titanium abutment, implant, and abutment screw received a 35-N preload. For the crown restorations, an 86% gold alloy (Aquarius; Ivoclar Vivadent AG, Schaan, Liechtenstein) was used as the material of the metal crown. The crown morphology was designed to imitate the maxillary second premolar, and the sizes were the same in each set of the model. The angles of inner inclination of the buccal and palatal cusps were designed to be 30° to the occlusal table. Abutment heights of the models were all modified to 5 mm from the crown margin to the top of the abutment. The fit between the abutment and the crown restoration was assumed to be intimate contact.²¹ The rough surface of the testing fixtures about 10 mm long were totally embedded in the bone, and interface conditions between the bone and

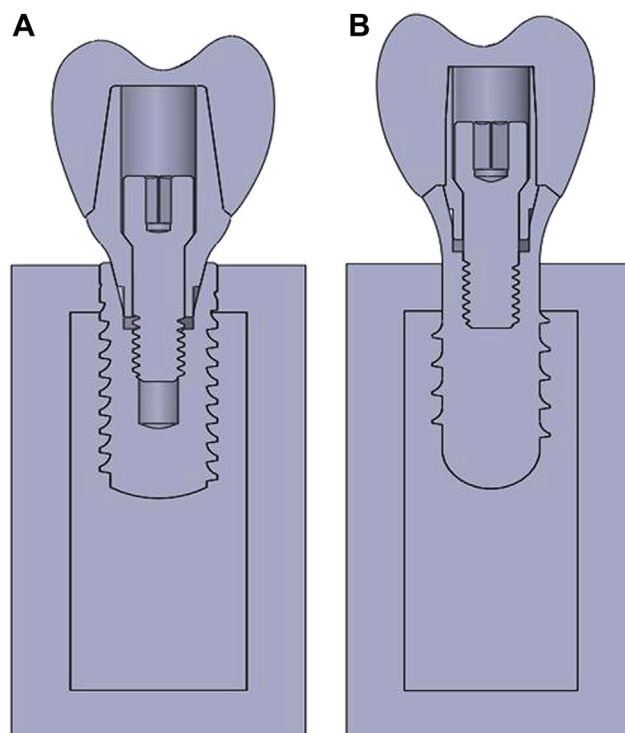


Figure 2 Plane diagram illustrating the model design and geometry of the Straumann implant with the rough surface totally embedded in bone. (A) Bone-leveled; (B) tissue-leveled.

implant were assumed to be fully osseointegrated. The crown margin to the crestal bone level was designed with the same distance of 1.8 mm (Fig. 1).

Model building and geometry

The bone model was simplified to a cuboid form (10 mm × 10 mm × 20 mm) and was classified as type II or IV bone; type II bone consisted of a layer of cortical bone with

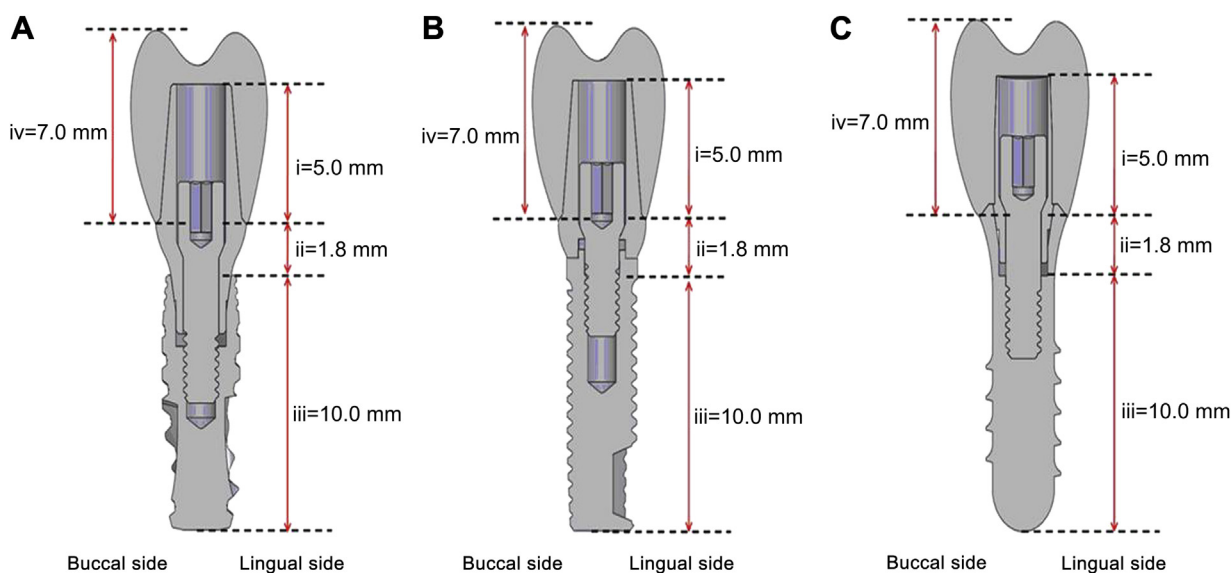


Figure 1 The model design of specimen components and interface condition of NobelBiocare and Straumann implants. (A) NobelBiocare bone-leveled; (B) NobelBiocare MK III tissue-leveled, and (C) Straumann tissue-leveled.

Table 2 Number of elements and nodes in the NobelBiocare system.

	Type II				Type IV			
	NobelBiocare							
	Active		MK III		Active		MK III	
	Element	Node	Element	Node	Element	Node	Element	Node
Crown	18,183	3868	18,644	3959	18,733	3963	18,644	3959
Abutment	8582	2200	8328	2114	8428	2172	8329	2115
Screw	5742	1403	5730	1402	5771	1407	5730	1402
Implant	49,524	10,484	22,154	5145	49,431	10,459	22,645	5262
Cortex	25,287	5553	25,152	5479	15,391	3829	14,602	3674
Cancellous	22,469	4882	25,056	5437	32,075	6733	35,788	7451

uniform thickness of 2 mm, which was surrounded by a core of dense trabecular bone, whereas type IV bone consisted of a thin layer cortical bone with uniform thickness 1 mm, surrounded by a core of loose trabecular bone (Fig. 2).²² The 3D models were built by SolidWorks computer aided design program, which is capable of input geometric features such as length, angle, diameter, and profile to make drawings of the sample parts and assemblies.

Elements and nodes

Eight finite element models were constructed with two implant systems, which contained four types of fixture in combination with two types of bone quality; the numbers of elements and nodes were well refined in the models (Tables 2 and 3). The refined mesh of the crown restoration, abutment, screw, implant, and cancellous bone were all set to an element size of 0.4 mm, whereas the crestal cortical bone was 1 mm (Fig. 3).

Finite element analyses

The finite element analyses were performed with the Abaqus 6.9 program, which was used to calculate the von Mises stress distribution. Computer-aided engineering software was used to input a 3D model of the sample and defined the mesh control of the models. After meshing the 3D model, conditions such as loads, constraints, and materials were assigned. A 100-N axial force and a 30° oblique

force were applied to the occlusal table of the crown restoration to analyze the stress distribution in the crown restoration, abutment, screw, implant, and supporting bone. The axial load was applied on the inner inclination of lingual cusp and buccal cusp with the same distance of 1.5 mm from the central developing groove, and an oblique load was applied to the inner inclination of the buccal cusp 2 mm from the central groove.

Results

The maximum von Mises stresses obtained are shown in Table 4 (NobelBiocare system) and Table 5 (Straumann system). The highest principal stresses were mostly found in the abutments in both systems, especially in an oblique loading situation. Descriptions of the maximum von Mises stresses were mainly according to the implant system and its related products.

Implant system

NobelBiocare system

For crown restorations, the maximum von Mises stresses were concentrated at the points of load application on the occlusal surfaces in both products in an oblique loading situation. However, the stress was greater with NobelActive (113.46 MPa) than with Brånemark MK III (70.13 MPa) in type II bone. For abutments, the maximum von Mises stresses were found in the oblique loading situation; they were

Table 3 Number of elements and nodes in the Straumann system.

	Type II				Type IV			
	Straumann							
	Bone level		Tissue level		Bone level		Tissue level	
	Element	Node	Element	Node	Element	Node	Element	Node
Crown	17,816	3836	18,817	3912	18,184	3925	18,172	3811
Abutment	6228	1643	3702	1164	6075	1620	4257	1384
Screw	5747	1398	5709	1398	5620	1380	5838	1417
Implant	17,657	4071	15,926	3696	17,752	4093	16,726	3883
Cortex	23,690	5165	23,707	5136	14,298	3561	14,625	3622
Cancellous	20,881	4494	20,287	4229	29,666	6148	30,282	6130

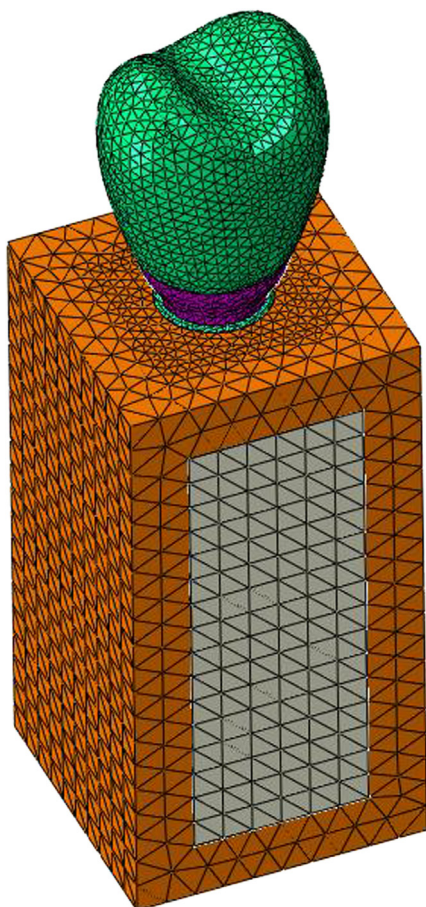


Figure 3 Three-dimensional view of elements and nodes distribution with different components of the model are illustrated. Key: Green = crown restoration; purple = abutment collar; blue = implant shoulder; brown = cortical bone; gray = cancellous bone.

2.7-times greater with Brånemark MK III (662.30 MPa) than with NobelActive (245.45 MPa) in type II bone, and 2.1-times greater with Brånemark MK III (583.53 MPa) than with NobelActive (274.20 MPa) in type IV bone. For screws, the maximum von Mises stresses were found in an oblique loading situation; they were 2.2-times greater with Brånemark MK III (200.19 MPa) than with NobelActive

(90.10 MPa) in type II bone and 2.1-times greater with Brånemark MK III (253.47 MPa) than with NobelActive (123.02 MPa) in type IV bone. In implants, the maximum von Mises stresses were found in an oblique loading situation, especially in type IV bone, and were 1.8 times greater in Brånemark MK III (463.49 MPa) than with NobelActive (254.64 MPa). For cortical bone, the maximum von Mises stresses were found in an oblique loading situation; they were 1.5-times greater with Brånemark MK III (97.07 MPa) than with NobelActive (66.51 MPa) in type II bone. For cancellous bone, the maximum von Mises stresses were found in an axial loading situation; they were 1.9-times greater with NobelActive (1.94 MPa) than with Brånemark MK III (0.99 MPa) in type II bone and 1.4-times greater with NobelActive (2.58 MPa) than with Brånemark MK III (1.84 MPa) in type IV bone.

Straumann system

For crown restorations, the maximum von Mises stresses were concentrated at the points of load application on the occlusal surfaces in both products in an oblique loading situation (Fig. 4). They were 3.2-times greater in the tissue-level implant (253.26 MPa) than the bone-level implant (80.72 MPa) in type II bone and also 3.2-times greater in the tissue-level implant (234.16 MPa) than the bone-level implant (73.68 MPa) in type IV bone. For abutments, the maximum von Mises stresses were found in an oblique loading situation; they were 4.8-times greater in the tissue-level implant (1203.04 MPa) than the bone-level implant (247.43 MPa) in type II bone and just 1.1-times greater in the tissue-level implant (359.13 MPa) than bone-level implant (324.54 MPa) in type IV bone. For screws, the maximum von Mises stresses were 1.6-times greater in the tissue-level implant (181.70 MPa) than the bone-level implant (116.20 MPa) in type IV bone. For implants, the maximum von Mises stresses were found in an oblique loading situation; they were 1.5-times greater in the tissue-level implant (339.82 MPa) than the bone-level implant (234.54 MPa) in type II bone and 1.6-times greater in the tissue-level implant (374.16 MPa) than the bone-level implant (240.88 MPa) in type IV bone. For cortical bone, the maximum von Mises stresses were found in an oblique loading situation; they were 1.6-times greater in the tissue-level implant (94.23 MPa) than the bone-level implant (57.53 MPa) in type II bone, and 1.7-times greater in the tissue-level implant

Table 4 Maximum von Mises stress (MPa) in different components of NobelBiocare models in different bone qualities and different loading angles.

Products	NobelBiocare							
	Type II				Type IV			
	Active		MK III		Active		MK III	
Loading angle	0°	30°	0°	30°	0°	30°	0°	30°
Crown	7.8686	113.4610	6.8723	70.1333	7.5512	84.5432	6.9873	70.2599
Abutment	13.3162	245.4520	26.7876	662.3030	13.8777	274.2010	28.3132	583.5320
Screw	9.6096	90.1041	16.1044	200.1940	12.1696	123.0210	18.1549	253.4690
Implant	15.1580	283.7150	14.1403	312.7180	23.6874	254.6440	16.7891	463.4930
Cortex	6.0839	66.5107	7.6799	97.0723	2.3523	20.9631	3.0124	20.6457
Cancellous	1.9425	5.0874	0.9989	3.9715	2.5809	7.9157	1.8429	8.2781

Table 5 Maximum von Mises stress (MPa) in different components of Straumann models in different bone qualities and different loading angles.

Products	Straumann							
	Type II				Type IV			
	Bone level		Tissue level		Bone level		Tissue level	
Loading angle	0°	30°	0°	30°	0°	30°	0°	30°
Crown	6.4455	80.7191	16.0696	253.2560	16.1588	73.6771	22.4397	234.1630
Abutment	12.6970	247.4260	85.4391	1203.0400	16.6552	359.1300	25.8439	382.8440
Screw	10.3743	96.3107	15.9071	210.7840	10.5059	116.1950	12.1518	181.6970
Implant	11.8742	234.5430	14.4268	339.8240	33.4159	240.8820	18.1096	374.1600
Cortex	8.7094	57.5333	7.6921	94.2295	33.8099	61.1688	11.2280	104.4830
Cancellous	0.7962	3.4723	1.3093	3.7415	1.0002	4.0189	1.2033	4.9687

(374.16 MPa) than the bone-level implant (240.88 MPa) in type IV bone. For cancellous bone, the maximum von Mises stresses were found in an oblique loading situation; they were 1.1-times greater in the tissue-level implant (3.74 MPa) than the bone-level implant (3.47 MPa) in type II bone, and 1.2-times greater in the tissue-level implant (4.97 MPa) than the bone-level implant with a convergent platform collar.

Bone-leveled implant with convergent platform collar

The maximum von Mises stresses in the bone-level implant with a platform design in cortical and cancellous bone with

different loading angles are illustrated in Fig. 5. The stress distribution in cortical bone also revealed that the higher the loading angle, the greater the von Mises stress distribution found in both implant systems, in either type II or type IV bone. Von Mises stresses in the Straumann system were mostly greater than those in the NobelBiocare system, except in type II bone with a 30° oblique loading angle. The maximum von Mises stresses in cancellous bone with the NobelBiocare system were greater than those of the Straumann system in relative bone types and loading angles.

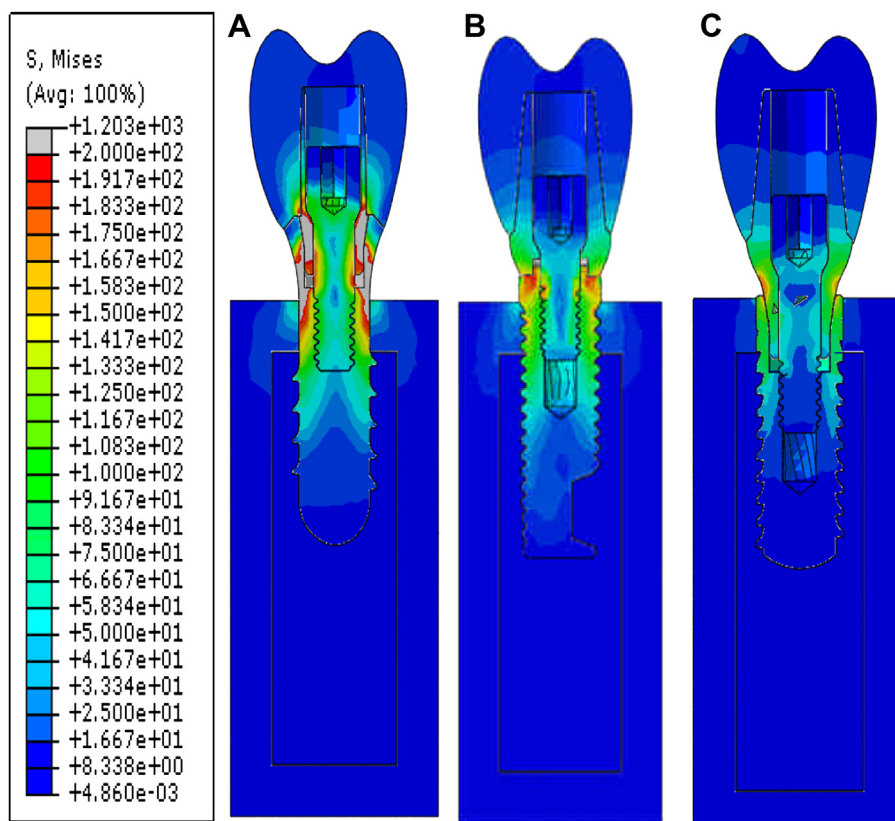


Figure 4 The stress concentrated in abutment and implant connection, especially in tissue-levelled implant of the Straumann system in type II bone under 30° loading angle. (A) Straumann tissue-levelled implant; (B) NobelBiocare MK III tissue-levelled implant; (C) Straumann bone-levelled implant.

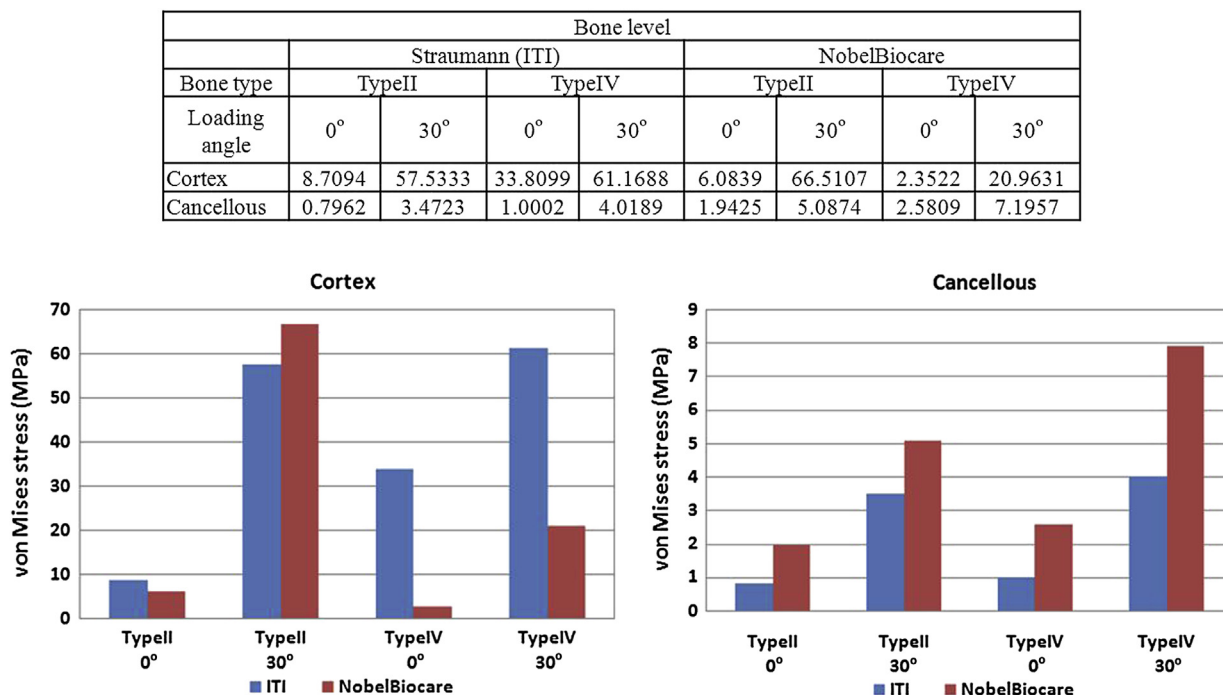


Figure 5 Table and diagrams illustrating the comparison of maximum von Mises stress (MPa) of bone-levelled implants of both implant systems in different bone qualities and loading angles.

Tissue-level implant with a straight and divergent margin connection

Results of the maximum von Mises stress analyses in the tissue-level implant with a straight and divergent design and with cortical and cancellous bone with different loading angles are shown in Fig. 6. The maximum von Mises stresses

in cortical bone in the Straumann system were mostly greater than those in the NobelBiocare system, except in type II bone with a 30° oblique loading angle. The maximum von Mises stresses in cancellous bone in the NobelBiocare system were greater than those in the Straumann system, except in type II bone with axial loading angle.

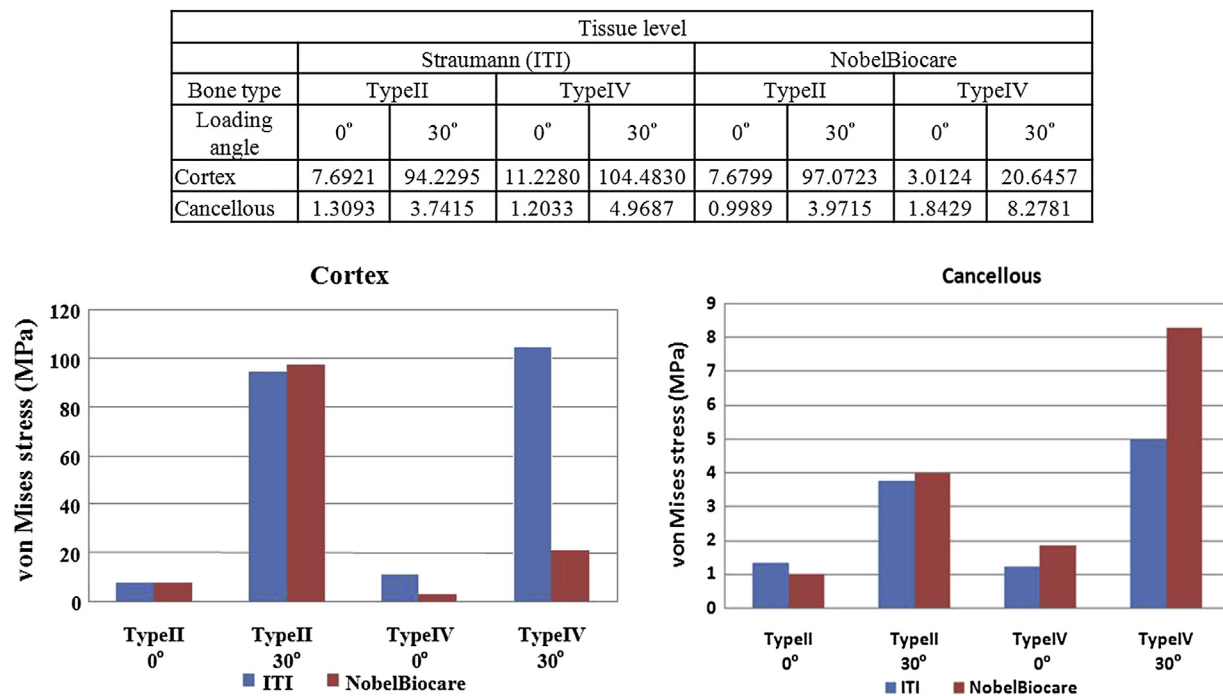


Figure 6 Table and diagrams illustrating the comparison of maximum von Mises (MPa) stress of tissue-levelled implants of both implant systems in different bone qualities and loading angles.

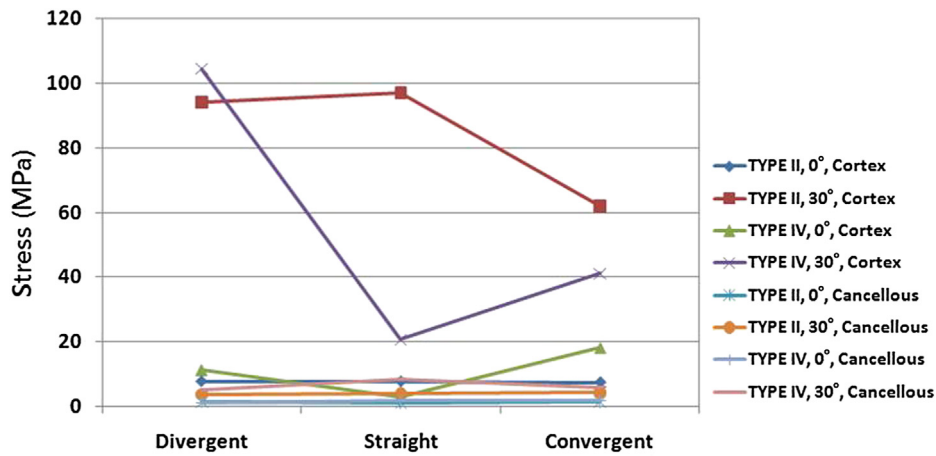


Figure 7 Comparison of stress distribution of implants with divergent, straight, and convergent collars in different bone qualities and loading angles.

Discussion

In spite of dental implants having successfully been used to replace missing teeth for decades, there are still many related complications in clinical performance, including porcelain fracture, screw loosening, fracture of implant

components, and surrounding bone resorption.^{23–26} However, veneer fracture of implant-supported restorations has become the most common complication of dental implant treatment, and it may shorten the longevity of prostheses.^{23,24} Small veneer fractures can be repaired, but larger fractures often require a new crown or bridge. Lateral

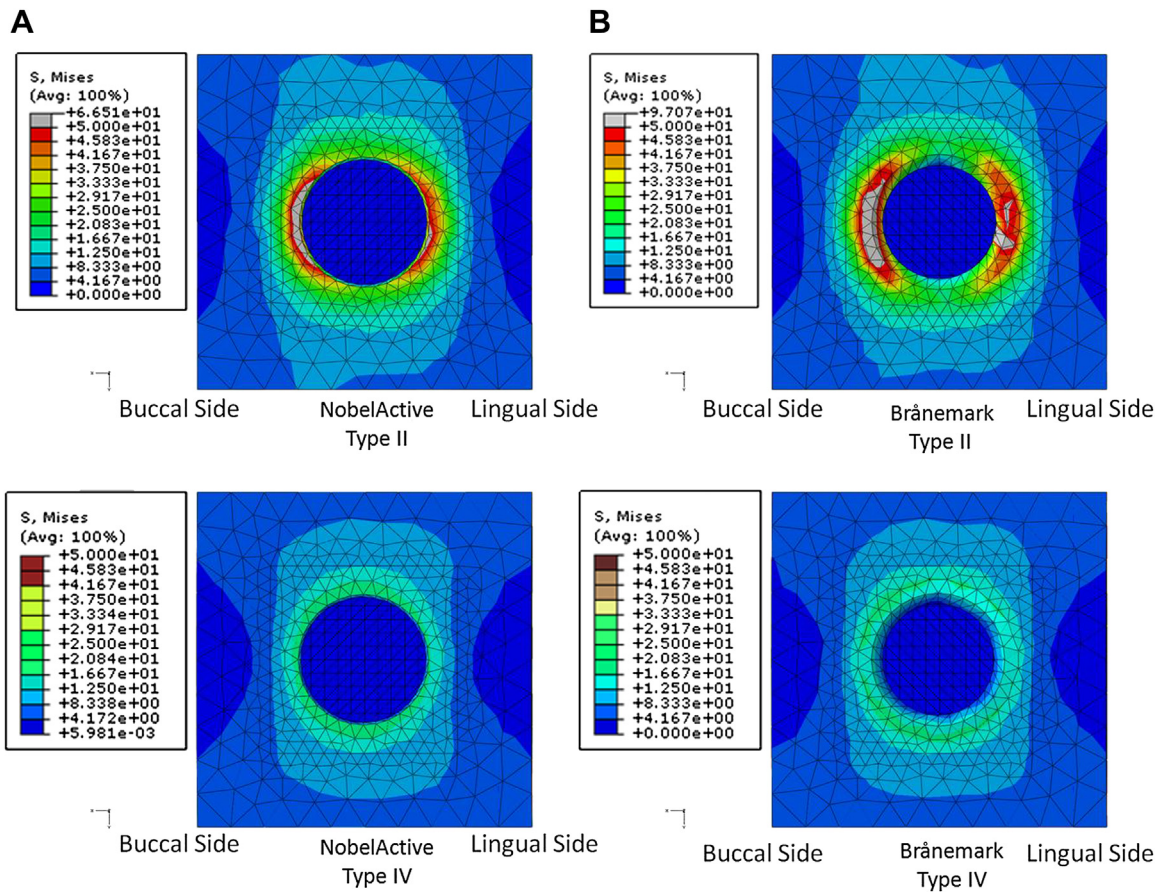


Figure 8 Occlusal view of stress distribution features on the top of the cortical bone crest surrounding the NobelBiocare implants in type II and type IV bone with 30° loading angle on the buccal side. Type II bone represents more stress concentrations on the buccal side of the cortical bone than on the lingual side. Bone-leveled implants (left) were less than tissue-levelled implants (right).

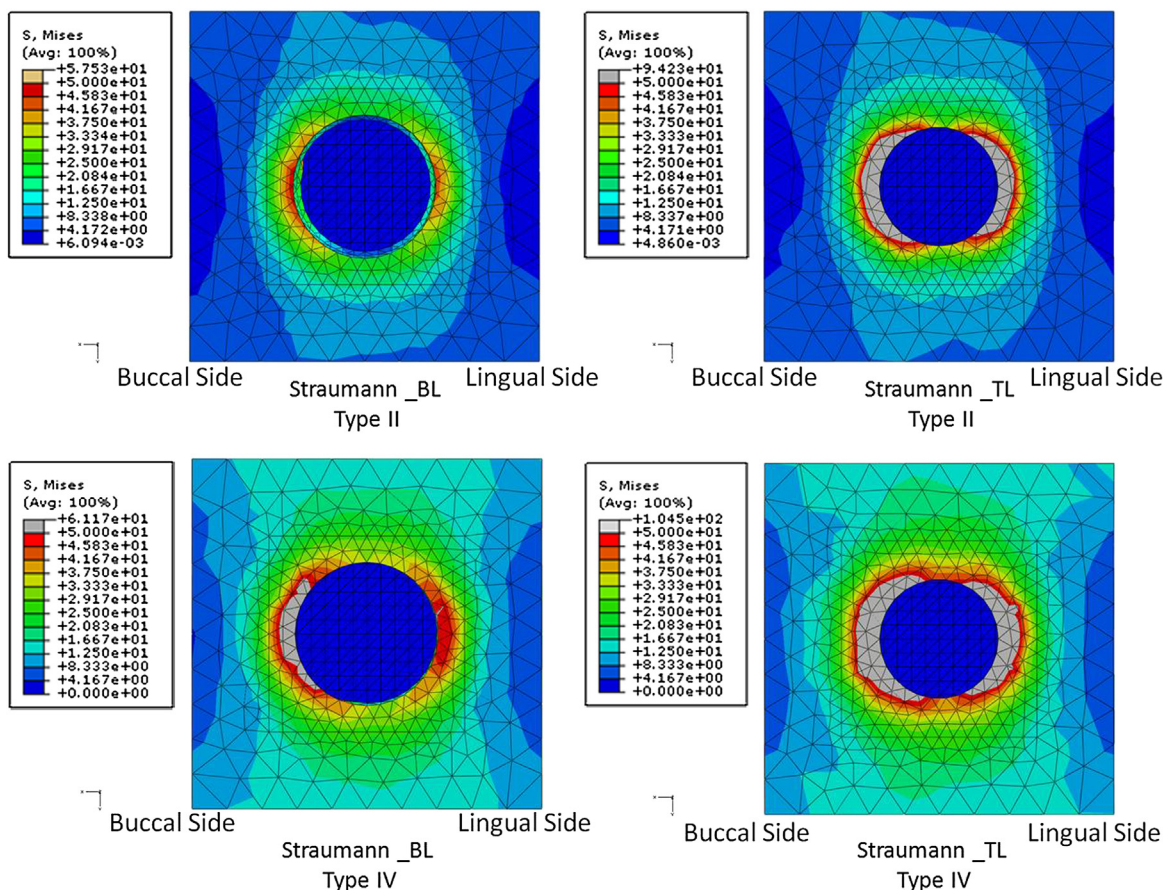


Figure 9 Occlusal view of stress distribution features on the top of the bone crest surrounding the Straumann implants in type II and type IV bone with 30° loading force on the buccal side. Type IV bone represents more stress concentrations on the buccal side of the bone crest than on the lingual side. Tissue-levelled implants were greater than bone-levelled implant. BL = bone-levelled; TL = tissue-levelled.

occlusal interference or unusual heavy biting forces may lead to fracture of veneer restorations and surrounding crestal bone resorption of the dental implant. The maximum von Mises stresses in crown restorations in the present study were about 10–16-times greater with a 30° loading angle in both systems. This implies that the tremendous stress and strain during premature contact or lateral occlusal interference can damage the veneer of implant-supported prostheses. Another important finding in this study was that the components of both implant systems seemed to bear most of the stresses that were mainly concentrated at the neck portion connection of the abutment-screw-implant complex, especially in tissue-levelled implant of Straumann system (1203.04 MPa) with the 30° loading angle (Fig. 4). These findings suggest that the tissue-level implant with a straight external hexagonal abutment connection of the NobelBiocare system may provide better clinical performance than the tissue-level implant with a divergent internal hexagonal abutment connection of the Straumann system in type II bone under a 30° loading angle situation. Fig. 4 also shows that the stress concentration shifted to the interface of the bone-level implant and minimized the stress in crestal cortical bone. By contrast, the tissue-level implant of the Straumann system seemed to be superior than that of the NobelBiocare

system in type IV bone with a 30° loading angle. However, clinical studies are necessary to confirm these findings. The final results also revealed that the bone-level implant with a convergent collar design possessed a better stress distribution than the tissue-level design of both systems. The implant and abutment of both systems inherited most of the stresses in both types of bone quality under a 30° loading angle (Figs. 5 and 6). Many clinical studies revealed that the greatest von Mises stresses were concentrated in the abutment-implant complex, which may be related to frequent complications, including screw loosening and abutment or retaining screw fracturing.^{27–29} The von Mises stresses in the abutment-implant complex in the present study were similar in both systems, which were consistent with the findings of those previous studies by Holmgren et al and Quaresma et al.^{30,31}

With the exception of analyzing the stress distributions in crown restorations and implant components, another important issue about the stress distribution in cortical bone and cancellous bone should be seriously discussed. Long-term success rates of dental implants suggest that soft and hard tissues surrounding an implant should be able to tolerate biological and mechanical irritation. In particular, the surrounding bone receives long-term nonaxial loading cycles, and bone fatigue may occur and cause weakening of

the bone structure, as reported previously.^{15,32–34} Excessive occlusal forces on implant-supported prostheses can impair osseointegration or induce bone resorption.^{7,35,36} The maximum von Mises stresses in the cortical bone surrounding the tissue-level implant were similar in both systems in type II and type IV bone, but with the exception of type IV bone, the Straumann system provided a better stress distribution.

Generally speaking, based on the results of this study, the maximum von Mises stresses in bone-level implant models with a convergent platform collar of both systems exhibited better results than tissue-level implant models with straight or divergent match margin connections in cortical bone, especially with a 30° loading angle (Figs. 5 and 6). The present results were consistent with the conclusions proposed by Bozkaya et al,³⁷ who suggested that implants with a convergent collar exhibited a favorable stress distribution at the top of cortical bone crest. The results were also consistent with those of Misch and Bidez³⁸ and Shen et al,¹⁶ who claimed that divergent collars were more favorable than straight collars in type II bone with a 30° loading angle. However, stress distributions of straight collars were more favorable than those of divergent collars in type IV cortical bone in this study (Fig. 7).

According to the findings of this study, the solitary implant design cannot be applicable for all bony situations. Stress distributions in type II cortical bone were similar to each other, whereas the NobelBiocare system expressed better than the Straumann system in type IV cortical bone. Most of the stress distributions were concentrated on the top of cortical bone for all of the models, especially under nonaxial loads (Figs. 8 and 9). Figs. 8 and 9 also show that stress concentration on the buccal side of the cortical bone was greater than that on the lingual side, and that of the tissue-level implant was greater than that of the bone-level implant. The abutment-implant connection on convergent collar implants was closer to the crestal cortical bone than implants with straight or divergent collars. In the present study, the divergent collar design seemed to transfer stresses to the internal abutment-implant connection, whereas stress concentrations at the abutment-implant junction may have increased the opportunity of loosening or fracturing the components of the dental implants. More clinical evidence is required to confirm the findings of the present study. In this study, the rough surface of the standard screw implants embedded in bone models was assumed to be close to each specimen, and we attempted to analyze the stress distribution on the bone surrounding the different implant collar designs with a 100-N loading force, which is within physiologic limits. However, nonaxial heavy biting forces usually far exceed this test force, which could exacerbate the stress concentration on the crestal cortical bone and cause saucerization of the supporting bone of dental implants in actual oral conditions. Maximum stress areas were numerically located at the abutment-implant connection, and a possible nonaxial overloading could occur in compression in cortical and cancellous bone.³⁹ Higher remodeling activity under nonaxial versus axial loads, also reported in an animal study,⁴⁰ was correlated with higher equivalent stresses in a finite element analysis study.⁴¹ In the present study, the

conditions between the implant and surrounding bone were assumed to be fully osseointegrated for all well-refined models. However, partial osseointegration usually occurs in actual clinical situations, and the screw design and rough surface of dental implants are usually dissimilar to each other, but all mathematical values were generated with the same loading and bony conditions in this study. Finite element models have limitations because the mechanical properties and the nonlinear behavior of biological tissues cannot precisely be imitated in the actual oral cavity. More clinical trials are necessary to confirm further the findings of the present study.

In conclusion, according to the results of the present study, the solitary implant design cannot be applicable for all bony situations. However, dental implants with a convergent (platform-switching) collar expressed better stress distributions than straight or divergent collars in cortical bone when under a 30° angle loading. In order to achieve favorable success rates or survival rates of dental implant treatment, careful selection of the implant system combined with ideal bone quality and a proper loading protocol are strongly suggested to minimize the destructive influence of loading forces on the surrounding bone of a dental implant.

Acknowledgments

This study was supported by the Veterans Affairs Commission, Executive Yuan, Taiwan. Technical support was provided by the Metal Industries Research and Development Center, Kaohsiung, Taiwan.

References

1. Sahin S, Cehreli MC, Yalçin E. The influence of functional forces on the biomechanics of implant-supported prostheses—a review. *J Dent* 2002;30:271–82.
2. Cehreli M, Sahin S, Akça K. Role of mechanical environment and implant design on bone tissue differentiation: current knowledge and future contexts. *J Dent* 2004;32:123–32.
3. Chee W, Jivraj S. Failures in implant dentistry. *Br Dent J* 2007; 202:123–9.
4. Hoshaw SJ, Brunski JB, Cochran GVB. Mechanical loading of Brånemark implants affects interfacial bone modeling and remodeling. *Int J Oral Maxillofac Implants* 1994;9:345–60.
5. Huang HM, Pan LC, Lee SY, Ho KN, Fan KH, Chen CT. Natural frequency analysis for the stability of a dental implant by finite element method. *J Med Biol Eng* 2001;21:61–7.
6. Jaffin RA, Berman CL. The excessive loss of Brånemark fixtures in type IV bone: a 5-year analysis. *J Periodontol* 1991;62:2–4.
7. Isidor F. Loss of osseointegration caused by occlusal load of oral implants. A clinical and radiographic study in monkeys. *Clin Oral Implants Res* 1996;7:143–52.
8. Miyata T, Kobayashi Y, Araki H, Ohto T, Shin K. The influence of controlled occlusal overload on peri-implant tissue. Part 3: a histologic study in monkeys. *Int J Oral Maxillofac Implants* 2000;15:425–31.
9. Becker J, Ferrari D, Herten M, Kirsch A, Schaer A, Schwarz F. Influence of platform switching on crestal bone changes at non-submerged titanium implants: a histomorphometrical study in dogs. *J Clin Periodontol* 2007;34:1089–96.
10. Cochran DL, Bosshardt DD, Grize L, Higginbottom FL, Jones AA, Jung RE, et al. Bone response to loaded implants with non-

- matching implant-abutment diameters in the canine mandible. *J Periodontol* 2009;80:609–17.
11. Luongo R, Traini T, Guidone PC, Bianco G, Cocchetto R, Celletti R. Hard and soft tissue responses to the platform-switching technique. *Int J Periodontics Restorative Dent* 2008;28:551–7.
 12. Vela-Nebot X, Rodriguez-Ciurana X, Rodado-Alonso C, Segalà-Torres M. Benefits of an implant platform modification technique to reduce crestal bone resorption. *Implant Dent* 2006;15:313–20.
 13. Prosper L, Redaelli S, Pasi M, Zarone F, Radaelli G, Gherlone EF. A randomized prospective multicenter trial evaluating the platform-switching technique for the prevention of post-restorative crestal bone loss. *Int J Oral Maxillofac Implants* 2009;24:299–308.
 14. Canullo L, Fedele GR, Iannello G, Jepsen S. Platform switching and marginal bone-level alterations: the results of a randomized-controlled trial. *Clin Oral Impl Res* 2010;21:115–21.
 15. Hsu ML, Chen FC, Kao HC, Cheng CK. Influence of off-axis loading of an anterior maxillary implant: a 3-dimensional finite element analysis. *Int J Oral Maxillofac Implants* 2007;22:301–9.
 16. Shen WL, Chen CS, Hsu ML. Influence of implant collar design on stress and strain distribution in the crestal compact bone: a three-dimensional finite element analysis. *Int J Oral Maxillofac Implants* 2010;25:901–10.
 17. Tada S, Stegaroiu R, Kitamura E, Miyakawa O, Kusakari H. Influence of implant design and bone quality on stress/strain distribution in bone around implants: a 3-dimensional finite element analysis. *Int J Oral Maxillofac Implants* 2003;18:357–68.
 18. Sevimay M, Turhan F, Kiliçarslan MA, Eskitascioglu G. Three-dimensional finite element analysis of the effect of different bone quality on stress distribution in an implant-supported crown. *J Prosthet Dent* 2005;93:227–34.
 19. Tepper G, Hass R, Zechner W, Krach W, Watzek G. Three-dimensional finite element analysis of implant stability in the atrophic posterior maxilla: A mathematical study of the sinus floor augmentation. *Clin Oral Implants Res* 2002;13:657–65.
 20. Craig RG. *Restorative Dental Materials*, 6th ed. St Louis: CV Mosby, 1980:286–7.
 21. Hojjatie B, Anusavice KJ. Three-dimensional finite element analysis of glass-ceramic dental crowns. *J Biomech* 1990;23:1157–66.
 22. Miyamoto I, Tsuboi Y, Wada E, Suwa H, Iizuka T. Influence of cortical bone thickness and implant length on implant stability at the time of surgery—clinical, prospective, biomechanical, and imaging study. *Bone* 2002;37:776–80.
 23. Goodacre CJ, Bernal G, Rungcharassaeng K, Kan JY. Clinical complications with implants and implant prostheses. *J Prosthet Dent* 2003;90:121–32.
 24. Nedir R, Bischof M, Szmukler-Moncler S, Belser UC, Samson J. Prosthetic complications with dental implants: from up-to-8-year experience in private practice. *Int J Oral Maxillofac Implants* 2006;21:919–28.
 25. Meijer HJA, Raghoobar GM, Batenburg RHK, Vissink A. Mandibular overdentures supported by two Brånemark, IMZ or Straumann implants: a ten-year prospective randomized study. *J Clin Periodontol* 2009;36:799–806.
 26. Simonis P, Dufour T, Tenenbaum H. Long-term implant survival and success: a 10-16-year follow-up of non-submerged dental implants. *Clin Oral Impl Res* 2010;21:772–7.
 27. Jemt T, Laney WR, Harris D, Henry PJ, Krogh Jr PH, Polizzi G, et al. Osseointegrated implants for single tooth replacement: a 1-year report from a multicenter prospective study. *Int J Oral Maxillofac Implants* 1991;6:29–36.
 28. Jemt T. Failure and complications in 391 consecutively inserted fixed prostheses supported by Brånemark implants in edentulous jaws: a study of treatment from the time of prosthesis placement to the first annual checkup. *Int J Oral Maxillofac Implants* 1991;6:270–6.
 29. Naert I, Quirynen M, van Sternberghe D, Darius P. A study of 589 consecutive implants supporting complete fixed prostheses. Part II: prosthetic aspects. *J Prosthet Dent* 1992;68:949–56.
 30. Holmgren EP, Seckinger RJ, Kilgren LM, Mante F. Evaluating parameters of osseointegrated dental implants using finite element analysis— a two-dimensional comparative study examining the effects of implant diameter, implant shape, and load direction. *J Oral Implantol* 1998;24:80–8.
 31. Quaresma ET, Cury R, Sendyk R, Sendyk C. A finite element analysis of two different dental implants: stress distribution in the prosthesis, abutment, and supporting bone. *J Oral Implantol* 2008;34:1–6.
 32. Gray RJ, Korbacher GK. Compressive fatigue behavior of bovine compact bone. *J Biomech* 1974;7:287–92.
 33. Swanson SA, Freeman MA, Day WH. The fatigue properties of human cortical bone. *Med Biol Eng* 1971;9:23–32.
 34. Burr DB, Forwood MR, Fyhrie DP, Martin RB, Schaffler MB, Turner CH. Bone microdamage and skeletal fragility in osteoporotic and stress fractures. *J Bone Miner Res* 1997;12:6–15.
 35. Isidor F. Histological evaluation of peri-implant bone at implants subjected to occlusal overload or plaque accumulation. *Clin Oral Implants Res* 1997;8:1–9.
 36. Quirynen M, Naert I, van Steenberghe D. Fixture design and overload influence marginal bone loss and fixture success in the Brånemark system. *Clin Oral Implants Res* 1992;3:104–11.
 37. Bozkaya D, Muftu S, Muftu A. Evaluation of load transfer characteristics of five different implants in compact bone at different load levels by finite elements analysis. *J Prosthet Dent* 2004;92:523–30.
 38. Misch CE, Bidez MW. A scientific rationale for dental implant design. In: Misch CE, ed. *Contemporary Implant Dentistry*, 2nd ed. St Louis: Mosby, 1999:329–43.
 39. Yoon KH, Kim SG, Lee JH, Suh SW. 3D finite element analysis of changes in stress levels and distributions for an osseointegrated implant after vertical bone loss. *Implant Dent* 2011;20:354–9.
 40. Barbier L, Schepers E. Adaptive bone remodeling around oral implants under axial and nonaxial loading conditions in the dog mandible. *Int J Oral Maxillofac Implants* 1997;12:215–23.
 41. Barbier L, Vander Sloten J, Krzesinski G, Schepers E, Van der Perre G. Finite element analysis of nonaxial versus axial loading of oral implants in the mandible of the dog. *J Oral Rehabil* 1998;25:847–58.